

Transition radiation on a dynamical periodical interface

A. R. Mkrtchyan^{1,2}, A. P. Potylitsyn^{2,3}, V. R. Kocharyan^{1,2}, A. A. Saharian¹

¹*Institute of Applied Problems in Physics,
25 Nersessian Street, 0014 Yerevan, Armenia*

²*Tomsk Polytechnic University, 30 Lenin Ave., 634050 Tomsk, Russia*

³*National Research Nuclear University MEPhI, 115409 Moscow, Russia*

March 16, 2016

Abstract

We investigate the transition radiation on a periodically deformed interface between two dielectric media. Under the assumption that the dielectric permittivities of the media are close, a formula is derived for the spectral-angular distribution of the radiated energy in the general case of a nonstatic profile function for the separating boundary. In particular, the latter includes the case of surface waves propagating along the boundary. The numerical examples are given for triangular grating and for sinusoidal profile. We show that instead of a single peak in the backward transition radiation on a flat interface, for periodic interface one has a set of peaks. The number and the locations of the peaks depend on the incidence angle of the charge and on the period of the interface. The conditions are specified for their appearance.

1 Introduction

The polarization of a medium by a moving charged particle gives rise to a number of radiation processes. Well-known examples are Cherenkov, transition and diffractions radiations. In particular, many aspects of transition radiation, both theoretical and experimental, have been investigated in numerous publications (for reviews see [1]). Transition radiation is produced when a relativistic particle traverses an inhomogeneous medium. Such radiation has a number of remarkable properties and at present it has found many important applications. In particular, optical and extreme ultraviolet transition radiation from metallic targets observed in backward direction was used for the measurement of transverse size, divergence and energy of electron and proton beams (see, for example, [2] and references therein).

The modern accelerators allow us to produce electron beams consisting of trains of short bunches with subpicosecond duration [3, 4]. The conventional diagnostic tools do not provide the required measurement accuracy and the development of new reliable and economic diagnostic techniques is the actual task. Such techniques based on different radiation mechanisms (for instance, transition radiation) are widely used [5]. Reconstruction of a bunch profile is carried out using the Fourier transformation of the measured spectrum of coherent transition radiation [6]. Recently a technique is proposed based on the Smith-Purcell radiation spectral measurements [7, 8]. The advantages of such kind of diagnostics are due to the fact that the Smith-Purcell radiation

spectral distribution is quasimonochromatic. But because of the weak radiation intensity the usage of the proposed technique meets with troubles [9]. We propose to use the transition radiation from periodically deformed targets instead of the Smith-Purcell radiation mechanism for beam diagnostic. In this case the radiation intensity is much higher but, as we show below, the spectral distribution becomes quasimonochromatic similar to the Smith-Purcell radiation and the abovementioned advantages are retained.

The main part of the investigations of transition radiation considers flat interfaces separating the media with different optical properties. Very few works have been devoted to the transition radiation from rough surfaces [10]. A periodic structure of the separating interface can serve as an additional tool for the control of the spectral-angular distribution of the transition radiation. In general, the problem does not allow an analytic solution and approximate or numerical methods should be used. An integral method to study transition radiation from interfaces with arbitrary profile was considered in [11]. The method is a generalization of that previously discussed in [12] for the case of the Smith-Purcell radiation. Relatively simple and physically more transparent expressions for the radiation intensity are obtained by using various approximations. In particular, the investigation of the transition radiation from regular-roughness interface is carried out in [13] under the assumption that the dielectric permittivities of the media separated by the interface are close to each other. The same approximation scheme has been used in [14] for the investigation of the radiation intensity from a charge or bunches flying over a surface waves.

In the present paper we consider the transition radiation on an interface with arbitrary periodic profile and for an arbitrary incidence angle of a charged particle. In particular, the function describing the profile can also be time dependent. This type of dynamical interface may be realized by surface waves propagating on the boundary of two media. The investigation will be done within the framework of the perturbation theory with respect to the small difference of the dielectric permittivities of the media. In particular, the corresponding condition is satisfied for the X-ray transition radiation. Another example is that when for a part of the medium the dielectric permittivity is changed by some external influences, for example, intense electromagnetic waves or acoustic waves. These changes are much smaller than the corresponding unperturbed permittivities and their effects are well described by the perturbation theory. Transition radiation on a superlattice created by acoustic waves has been discussed previously in [15]. The above-mentioned perturbation theory in general form with a number of applications is reviewed in [16]. The corresponding results can in certain cases be used to estimate the effects in more complicated configurations.

The paper is organized as follows. In the next section we obtain the formula for the spectral-angular density of the radiated energy for a general profile function. The formulas are given for separate polarizations, as well as for the total intensity. Special cases, which include diffraction gratings and surface waves excited on the interface, are discussed in section 3. Numerical examples for the both angular and spectral distributions of the radiated energy are considered in section 4. The main results are summarized in section 5.

2 Transition radiation for a general case of the profile function

First let us consider the general case of a medium with dielectric permittivity

$$\varepsilon = \varepsilon_0 + \Delta\varepsilon(\mathbf{r}, t), \quad (1)$$

where ε_0 is a constant and $|\Delta\varepsilon(\mathbf{r}, t)| \ll |\varepsilon_0|$. Let us denote by \mathbf{E}_0 and \mathbf{H}_0 the electric and magnetic fields created by the radiation source in a homogeneous medium with permittivity ε_0 .

Presenting the corresponding fields in the medium with permittivity (1) in the form $\mathbf{E} = \mathbf{E}_0 + \Delta\mathbf{E}$ and $\mathbf{H} = \mathbf{H}_0 + \Delta\mathbf{H}$ and substituting into the Maxwell equations, we can see that, in the first approximation with respect to the small quantity $|\Delta\varepsilon(\mathbf{r}, t)/\varepsilon_0|$, the fields $\Delta\mathbf{E}$ and $\Delta\mathbf{H}$ obey the inhomogeneous Maxwell equations with the charge density $\rho = \text{div}(\Delta\varepsilon\mathbf{E}_0)/(4\pi)$ and current density $j = \partial_t(\Delta\varepsilon\mathbf{E}_0)/(4\pi)$. Consequently, in the same approximation, the spectral-angular distribution of the radiated energy is given by the formula [16, 17]

$$W_\omega d\omega d\Omega = \frac{(2\pi)^4 \omega^4 \sqrt{\varepsilon_0}}{4c^3} \sum_{l=1}^2 |\mathbf{e}^l (\Delta\varepsilon\mathbf{E}_0)_{\mathbf{k}, \omega}|^2 d\omega d\Omega, \quad (2)$$

where \mathbf{e}^l , $l = 1, 2$, are independent unit vectors of the polarization, ω and \mathbf{k} are the frequency and wave vector of the radiated photon, $k = |\mathbf{k}| = \omega\sqrt{\varepsilon}/c$, $d\Omega$ is the solid angle element. In (2),

$$(\Delta\varepsilon\mathbf{E}_0)_{\mathbf{k}, \omega} = \int \frac{dtd\mathbf{r}}{(2\pi)^4} e^{-i(\mathbf{k}\mathbf{r} - \omega t)} \Delta\varepsilon(\mathbf{r}, t) \mathbf{E}_0(\mathbf{r}, t), \quad (3)$$

and the separate terms in the sum over l give the radiated energy for the corresponding polarization.

The Fourier transform appearing in (2) is expressed in terms of the Fourier transforms of the separate factors as

$$(\Delta\varepsilon\mathbf{E}_0)_{\mathbf{k}, \omega} = \int d\omega' d\mathbf{k}' \Delta\varepsilon(\mathbf{k} - \mathbf{k}', \omega - \omega') \mathbf{E}_0(\mathbf{k}', \omega'), \quad (4)$$

where

$$\Delta\varepsilon(\mathbf{k}, \omega) = \int \frac{dtd\mathbf{r}}{(2\pi)^4} e^{-i(\mathbf{k}\mathbf{r} - \omega t)} \Delta\varepsilon(\mathbf{r}, t). \quad (5)$$

For a point charge q moving with a constant velocity \mathbf{v} along the trajectory given by $\mathbf{r} = \mathbf{r}_0 + \mathbf{v}(t - t_0)$, the Fourier transform of the corresponding electric field is determined by the expression

$$\mathbf{E}_0(\mathbf{k}, \omega) = \frac{4\pi i q}{(2\pi)^3} \frac{\omega \mathbf{v}/c^2 - \mathbf{k}/\varepsilon_0}{k^2 - \omega^2 \varepsilon_0/c^2} e^{-i(\mathbf{k}\mathbf{r}_0 - \omega t_0)} \delta(\omega - \mathbf{k}\mathbf{v}). \quad (6)$$

In the present paper we consider the transition radiation on the boundary of two homogeneous media with dielectric permittivities ε_0 and ε_1 . For a general case of dynamical boundary the corresponding equation can be written as

$$x = x_0(y, z, t). \quad (7)$$

Here and below (x, y, z) stand for the Cartesian coordinates. Hence, in the problem under consideration the dielectric permittivity is given by

$$\varepsilon = \begin{cases} \varepsilon_0, & x < x_0(y, z, t), \\ \varepsilon_1, & x > x_0(y, z, t). \end{cases} \quad (8)$$

For the function $\Delta\varepsilon(\mathbf{r}, t)$ in (1) one can take

$$\Delta\varepsilon(\mathbf{r}, t) = \Delta\varepsilon \theta(x - x_0(y, z, t)), \quad \Delta\varepsilon = \varepsilon_1 - \varepsilon_0, \quad (9)$$

where $\theta(x)$ is the Heaviside unit step function. Assuming that $|\Delta\varepsilon|/\varepsilon_0 \ll 1$, for the Fourier transform (4), under the condition $\omega \neq \mathbf{k}\mathbf{v}$, one gets

$$\begin{aligned} (\Delta\varepsilon\mathbf{E}_0)_{\mathbf{k}, \omega} &= \frac{4\pi q}{(2\pi)^7} \int d\mathbf{k}' \frac{\Delta\varepsilon(\mathbf{k}'\mathbf{v})}{K_x} \frac{\mathbf{v}/c^2 - \mathbf{k}'/\varepsilon_0}{k'^2 - (\mathbf{k}'\mathbf{v})^2 \varepsilon_0/c^2} e^{-i\mathbf{k}'(\mathbf{r}_0 - \mathbf{v}t_0)} \\ &\times \int dt dy dz e^{i((\omega - \mathbf{k}'\mathbf{v})t + K_y y + K_z z)} e^{iK_x x_0(y, z, t)}, \end{aligned} \quad (10)$$

where

$$\mathbf{K} = \mathbf{k}' - \mathbf{k}. \quad (11)$$

For $\omega = \mathbf{k}\mathbf{v}$ an additional term is present in the expression for $(\Delta\varepsilon\mathbf{E}_0)_{\mathbf{k},\omega}$ containing the factor $\delta(\omega - \mathbf{k}\mathbf{v})$. This term gives contribution to the radiation along the Cherenkov angle only, if the corresponding condition is satisfied.

Assuming that the function $x_0(y, z, t)$ is periodic with the periods L_y , L_z , and T , for the function in the integrand of (10) we can write the Fourier expansion

$$e^{iK_x x_0(y,z,t)} = \sum_{m,n,l=-\infty}^{+\infty} f_{mnl}(K_x) e^{2\pi i(my/L_y + nz/L_z) - i\omega_l t}, \quad (12)$$

where $\omega_l = 2\pi l/T$, and

$$f_{mnl}(K_x) = \frac{1}{L_y L_z T} \int_0^{L_y} dy \int_0^{L_z} dz \int_0^T dt e^{iK_x x_0(y,z,t)} e^{-2\pi i(my/L_y + nz/L_z) + i\omega_l t}. \quad (13)$$

Substituting the expansion (12) into (10) one gets

$$(\Delta\varepsilon\mathbf{E}_0)_{\mathbf{k},\omega} = \frac{2q\Delta\varepsilon}{(2\pi)^3 v_x \varepsilon_0} \sum_{m,n,l=-\infty}^{+\infty} \frac{f_{mnl}(K_x)}{K_x} \frac{\mathbf{k}' - (\omega - \omega_l) \mathbf{v} \varepsilon_0 / c^2}{k'^2 - (\omega - \omega_l)^2 \varepsilon_0 / c^2} e^{-i\mathbf{k}'(\mathbf{r}_0 - \mathbf{v}t_0)}, \quad (14)$$

with the notations

$$\begin{aligned} \mathbf{k}' &= \mathbf{k} + K_x \mathbf{e}_x - \mathbf{g}, \\ K_x &= \frac{1}{v_x} (\omega - \mathbf{k}\mathbf{v} - \omega_l + \mathbf{g}\mathbf{v}), \\ \mathbf{g} &= (0, 2\pi m/L_y, 2\pi n/L_z), \end{aligned} \quad (15)$$

where \mathbf{e}_x is the unit vector along the x -axis. Note that we have the relation

$$\mathbf{k}'\mathbf{v} = \omega - \omega_l. \quad (16)$$

Let us denote the angle between the vectors \mathbf{v} and \mathbf{k} by θ_0 . Then, for the polarization vectors of the parallel and perpendicular polarizations one has

$$\mathbf{e}^1 = \mathbf{e}^{\parallel} = \frac{\mathbf{v} - (\mathbf{n}\mathbf{v})\mathbf{n}}{v \sin \theta_0}, \quad \mathbf{e}^2 = \mathbf{e}^{\perp} = \frac{\mathbf{n} \times \mathbf{v}}{v \sin \theta_0}, \quad (17)$$

where $\mathbf{n} = \mathbf{k}/k$ is the unit vector along the radiation direction. For the corresponding spectral-angular densities of the radiated energy one has

$$W_{\omega}^p = \frac{(2\pi)^4 \omega^4 \sqrt{\varepsilon_0}}{4c^3} |\mathbf{e}^p (\Delta\varepsilon\mathbf{E}_0)_{\mathbf{k},\omega}|^2, \quad (18)$$

with $p = \parallel$ and $p = \perp$. The expression for the total spectral-angular density takes the form

$$W_{\omega} = W_{\omega}^{\parallel} + W_{\omega}^{\perp} = \frac{(2\pi)^4 \omega^4 \sqrt{\varepsilon_0}}{4c^3} \left[|(\Delta\varepsilon\mathbf{E}_0)_{\mathbf{k},\omega}|^2 - |(\mathbf{n}(\Delta\varepsilon\mathbf{E}_0)_{\mathbf{k},\omega})|^2 \right]. \quad (19)$$

Note that we can also write

$$|(\Delta\varepsilon\mathbf{E}_0)_{\mathbf{k},\omega}|^2 - |(\mathbf{n}(\Delta\varepsilon\mathbf{E}_0)_{\mathbf{k},\omega})|^2 = |\mathbf{n} \times (\Delta\varepsilon\mathbf{E}_0)_{\mathbf{k},\omega}|^2. \quad (20)$$

Substituting the expression (14) into (18) and assuming that the beam cross section is larger than the periods L_y and L_z , for the spectral-angular densities of the radiated energy on separate polarizations, averaged over the impact parameter, one gets the expression

$$W_\omega^p = \frac{q^2 (\Delta\varepsilon)^2 \omega^4}{4\pi^2 c^3 \varepsilon_0^{3/2} v_x^2 v^2 \sin^2 \theta_0} \sum_{m,n,l=-\infty}^{+\infty} \frac{V_p |f_{mnl}(K_x)|^2 / K_x^2}{[\omega_l(2\omega - \omega_l)\varepsilon_0/c^2 + K_x^2 + \mathbf{g}^2 + 2(k_x K_x - \mathbf{k}\mathbf{g})]^2}, \quad (21)$$

where for the parallel and perpendicular polarizations we have

$$\begin{aligned} V_\parallel &= \{(\omega - \omega_l)(1 - \beta_0^2) - (\mathbf{n}\mathbf{v})[\omega\sqrt{\varepsilon_0}/c + n_x K_x - \mathbf{n}\mathbf{g} - (\omega - \omega_l)(\mathbf{n}\mathbf{v})\varepsilon_0/c^2]\}^2, \\ V_\perp &= ([\mathbf{n} \times \mathbf{v}] \cdot (K_x \mathbf{e}_x - \mathbf{g}))^2, \end{aligned}$$

with the notation $\beta_0 = v\sqrt{\varepsilon_0}/c$. The spectral-angular density for the total radiation is given by the formula

$$W_\omega = \frac{q^2 (\Delta\varepsilon)^2 \omega^4}{(2\pi)^2 c^3 v_x^2 \varepsilon_0^{3/2}} \sum_{m,n,l=-\infty}^{+\infty} \frac{V |f_{mnl}(K_x)|^2 / K_x^2}{[\omega_l(2\omega - \omega_l)\varepsilon_0/c^2 + K_x^2 + \mathbf{g}^2 + 2(k_x K_x - \mathbf{k}\mathbf{g})]^2}, \quad (22)$$

with the function

$$\begin{aligned} V &= K_x^2 + \mathbf{g}^2 - [(2 - \beta_0^2)(\omega - \omega_l) - 2(\mathbf{k}\mathbf{v})](\omega - \omega_l)\varepsilon_0/c^2 \\ &\quad - [K_x n_x - \mathbf{n}\mathbf{g} - (\omega - \omega_l)\mathbf{n}\mathbf{v}\varepsilon_0/c^2]^2. \end{aligned} \quad (23)$$

The presented formulas are valid in the first approximation with respect to the ratio $\Delta\varepsilon/\varepsilon_0$, for both backward and inward radiations. An additional condition, that is obtained comparing with the exact expressions in the case of flat boundary, is given below in section 3.

Special cases of the profile function for the interface and numerical examples will be discussed below. However, some features can be seen from general formulas. The spectral-angular density of the radiated energy contains the square of the vector (see (14))

$$\mathbf{A}(\mathbf{k}') = \frac{\mathbf{k}' - (\omega - \omega_l)\mathbf{v}\varepsilon_0/c^2}{k'^2 - (\omega - \omega_l)^2 \varepsilon_0/c^2}. \quad (24)$$

Introducing the angle θ' between the vectors \mathbf{k}' and \mathbf{v} and by taking into account the relation (16), we can see that

$$|\mathbf{A}(\mathbf{k}')|^2 = \frac{1 - (2 - \beta_0^2)\beta_0^2 \cos^2 \theta'}{k'^2 (1 - \beta_0^2 \cos^2 \theta')^2}. \quad (25)$$

From here it follows that if β_0^2 is close to 1, $|1 - \beta_0^2| \ll 1$, peaks can appear in the spectral angular distribution of the radiated energy for small values of the angle θ' . At these peaks one has

$$|\mathbf{A}(\mathbf{k}')|^2 \approx \frac{\theta'^2 \gamma_0^4}{k'^2 (1 + \gamma_0^2 \theta'^2)^2}, \quad (26)$$

where $\gamma_0^2 = 1/(1 - \beta_0^2)$, $|\gamma_0^2| \gg 1$. For $\varepsilon_0 = 1$ the parameter γ_0 coincides with the gamma factor of the radiating particle. One has $\theta' \sim 1/\gamma_0$ and the spectral-angular density at the peaks increases with increasing energy as γ_0^2 . The integration over the angle will give an additional factor θ' and the spectral density at the peaks increases as γ_0 .

The condition for the angle θ' to be small can be translated in terms of the wave vector of the radiated photon as

$$(\mathbf{k} - \mathbf{g} - \frac{\omega - \omega_l}{v^2} \mathbf{v}) \times \mathbf{e}_x = \mathcal{O}(1/\gamma_0^2). \quad (27)$$

This condition determines the location of possible peaks in the spectral-angular density of the radiated energy up to the terms of the order $1/\gamma_0^2$. Examples of this type of peaks will be given below. Note that the condition (27) does not depend on the form of the profile function and is completely determined by the periodicity properties of the interface.

In deriving the expressions for the spectral-angular distribution of the radiation intensity we have assumed that the charge of the radiating particle is fixed. New features may arise in the case of the transition radiation from multiply charged ions. In particular, as a result of the interaction with medium the ion can gain or lose charge. The transition radiation on a flat interface, by taking into account this effect, has been recently discussed in [18]. It has been shown that the change in the charge of the particle can lead to a considerable increase of the radiation intensity.

3 Special cases

As a check of the general formulas given above, first let us consider the case of a flat boundary between the media. In this case one has $x_0(y, z, t) = x_0 = \text{const}$ and the x -axis is perpendicular to the boundary. By taking into account that $f_{mnl}(K_x) = \delta_{m0}\delta_{n0}\delta_{l0}e^{iK_x x_0}$ and introducing the angles θ_v and θ in accordance with $v_x = v \cos \theta_v$ and $k_x = k \cos \theta$, for the spectral angular density of the radiated energy we get

$$W_{\omega}^{(\text{flat})} = \frac{q^2 (\Delta\varepsilon)^2 v^2 \cos^2 \theta_v w^2 - (2w - \beta_0^2) \beta_0^2 \cos^2 \theta_v - (w \cos \theta - \beta_0^2 \cos \theta_v \cos \theta_0)^2}{(2\pi)^2 c^3 \varepsilon_0^{3/2} w^4 (w + 2\beta_0 \cos \theta_v \cos \theta)^2}, \quad (28)$$

where

$$w = 1 - \beta_0 \cos \theta_0. \quad (29)$$

The special case of normal incidence is obtained taking $\theta_v = \pi$, $\theta = \pi - \theta_0$. It can be seen that (28) coincides with the exact formula in the limit when $\Delta\varepsilon$ is small and, additionally, under the conditions

$$|\Delta\varepsilon/\varepsilon_0| \ll \cos^2 \theta, \quad |\Delta\varepsilon/\varepsilon_0| \ll |(1 - \beta_0 \cos \theta_0) \cos \theta / \cos \theta_v|. \quad (30)$$

In particular, from these conditions it follows that the expressions given above are not valid for the radiation propagating nearly parallel to the interface (the angle θ is close to $\pi/2$). Limiting formulas, similar to (28), can also be obtained for the densities of separate polarizations.

Note that for the $l = m = n = 0$ term in the general formula (22) we have

$$W_{\omega}(l = m = n = 0) = |f_{000}(K_x)|^2 W_{\omega}^{(\text{flat})}. \quad (31)$$

By taking into account that $|f_{000}(K_x)|^2 \leq 1$, we conclude that the corresponding contribution to the radiation cannot exceed $W_{\omega}^{(\text{flat})}$. In the case of a flat interface and in the limit $|1 - \beta_0| \ll 1$, the peaks in the spectral-angular distribution of the radiation are realized for small angles θ_0 and near the angle for which the factor $(w + 2\beta_0 \cos \theta_v \cos \theta)^2$ in the denominator of (28) takes its minimal value. The first one corresponds to the peak in the forward radiation located near the particle velocity and the second one corresponds to the direction of specular reflection ($\theta = \pi - \theta_v$, $\theta_0 = \pi - 2\theta$).

Now we turn to the case of the profile function

$$x_0(y, z, t) = x_0(z - v_s t), \quad (32)$$

where the function $x_0(u)$ is periodic with the period L . Note that the function (32) describes a running surface wave with the wavelength L and velocity $v_s = L/T$. In this case for the

corresponding function $f_{mnl}(K_x)$ one has

$$f_{mnl}(K_x) = \delta_{m0}\delta_{nl}f_l(K_x), \quad (33)$$

with

$$f_l(K_x) = \frac{1}{L} \int_0^L dz e^{iK_x x_0(z) - 2\pi i l z/L}. \quad (34)$$

The corresponding radiation intensities are given by the expressions (21) and (22) with the replacements

$$\sum_{m,n,l=-\infty}^{+\infty} \rightarrow \sum_{l=-\infty}^{+\infty}, \quad f_{mnl}(K_x) \rightarrow f_l(K_x), \quad (35)$$

and with

$$\mathbf{g} = g_l \mathbf{e}_z = (0, 0, g_l), \quad g_l = 2\pi l/L, \quad (36)$$

where \mathbf{e}_z is the unit vector along the z -axis.

Introducing spherical angular coordinates for the vectors \mathbf{k} and \mathbf{v} ,

$$\begin{aligned} \mathbf{k} &= \frac{\omega}{c} \sqrt{\varepsilon_0} (\cos \theta, \sin \theta \sin \phi, \sin \theta \cos \phi), \\ \mathbf{v} &= v (\cos \theta_v, \sin \theta_v \sin \phi_v, \sin \theta_v \cos \phi_v), \end{aligned} \quad (37)$$

the spectral-angular density of the radiated energy on separate polarizations, for the profile function (32), are presented as

$$W_\omega^p = \frac{q^2 (\Delta\varepsilon)^2 v^2 \varepsilon_0^{-3/2}}{4\pi^2 c^3 \cos^2 \theta_v \sin^2 \theta_0} \sum_{l=-\infty}^{+\infty} \frac{U_p^2 |f_l(\omega K/v)|^2}{K^2 U^2}, \quad (38)$$

with the notations

$$K = \frac{1}{\cos \theta_v} \left(1 - \beta_0 \cos \theta_0 - \frac{\omega_l}{\omega} + \frac{v g_l}{\omega} \sin \theta_v \cos \phi_v \right), \quad (39)$$

and

$$\begin{aligned} U &= \frac{\omega_l}{\omega} \left(2 - \frac{\omega_l}{\omega} \right) \beta_0^2 + K^2 + \frac{v^2}{\omega^2} g_l^2 + 2\beta_0 \left(K \cos \theta - \frac{v g_l}{\omega} \sin \theta \cos \phi \right), \\ U_{\parallel} &= \left(1 - \frac{\omega_l}{\omega} \right) (1 - \beta_0^2) - \cos \theta_0 \left[\beta_0 + K \cos \theta - \frac{v g_l}{\omega} \sin \theta \cos \phi - \beta_0^2 \left(1 - \frac{\omega_l}{\omega} \right) \cos \theta_0 \right], \\ U_{\perp} &= [\mathbf{n} \times \mathbf{v}/v] \cdot (K \mathbf{e}_x - (v g_l/\omega) \mathbf{e}_z). \end{aligned} \quad (40)$$

For the total density we get

$$W_\omega = \frac{q^2 (\Delta\varepsilon)^2 v^2 \varepsilon_0^{-3/2}}{4\pi^2 c^3 \cos^2 \theta_v} \sum_{l=-\infty}^{+\infty} \frac{U_t |f_l(\omega K/v)|^2}{K^2 U^2}, \quad (41)$$

where

$$\begin{aligned} U_t &= K^2 + \frac{v^2 g_l^2}{\omega^2} - \left[(2 - \beta_0^2) \left(1 - \frac{\omega_l}{\omega} \right) - 2\beta_0 \cos \theta_0 \right] \left(1 - \frac{\omega_l}{\omega} \right) \beta_0^2 \\ &\quad - \left[K \cos \theta - \frac{v g_l}{\omega} \sin \theta \cos \phi - \left(1 - \frac{\omega_l}{\omega} \right) \beta_0^2 \cos \theta_0 \right]^2. \end{aligned} \quad (42)$$

Note that $v g_l/\omega = \beta_0 l \lambda/L$, where λ is the radiation wavelength. In the case of a surface wave one has $\omega_l = l \omega_s$, with $\omega_s = 2\pi/T$ being the frequency of the surface wave. For the radiation

on frequencies $\omega \gg \omega_s$, the terms containing the ratio ω_l/ω can be omitted and the spectral-angular densities coincide with the ones for the radiation on a static interface with the same profile function.

Let us denote by a the amplitude of the profile function $x_0(z)$. We can estimate the dependence of the radiation intensity on a , for large values of the ratio a/λ , by applying the stationary phase method to the integral (34). If the function $x_0(z)$ has an stationary point at $z = z_0$, $x'_0(z_0) = 0$, then for $a/\lambda \gg 1$ the dominant contribution comes from the region of the integration near that point. In this case one has $f_l(\omega K/v) \propto \sqrt{\lambda/a}$ and for large amplitudes the spectral-angular density decays as $1/a$. If the function $x_0(z)$ has no stationary point then $f_l(\omega K/v) \propto \lambda/a$ and the spectral-angular density behaves as $1/a^2$. For small values of the amplitude, $a/\lambda \ll 1$, the dominant contribution to the radiation intensity comes from the $l = 0$ term. The leading term coincides with the corresponding quantity for a flat boundary. The contributions from the terms $l \neq 0$ are suppressed by the factor $(a/\lambda)^2$.

The special case of the profile function (32) with $v_s = 0$ ($T \rightarrow \infty$ for a fixed L) corresponds to a static periodic interface with the period L . In this case one has $\omega_l = 0$. As an example of the separating boundary let us consider a triangular grating with the parameters displayed in figure 1. The corresponding profile function has the form

$$x_0(z) = \begin{cases} \frac{a}{b}(z - z_0), & z_0 \leq z \leq z_0 + b \\ \frac{a}{L-b}(z_0 + L - z), & z_0 + b \leq z \leq z_0 + L. \end{cases} \quad (43)$$

With this function, for the Fourier transform (34) we obtain the following expression

$$f_l(K_x) = 2e^{iK_x a/2 - \pi i l(2z_0 + b)/L} \frac{K_x a \sin(K_x a/2 - g_l b/2)}{(K_x a - g_l b)(K_x a - g_l b + 2\pi l)}. \quad (44)$$

For large values of the amplitude a , the function $|f_l(K_x)|^2$ decays as $1/a^2$. This agrees with the general estimate given above, by taking into account that the function (43) has no stationary point.

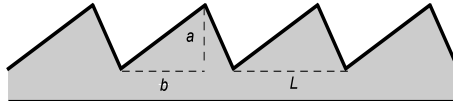


Figure 1: Parameters of the triangular grating.

As a next example of the profile function we consider a sinusoidal surface wave

$$x_0(z - v_s t) = a \sin(k_s z - \omega_s t), \quad (45)$$

where $v_s = \omega_s/k_s$, $k_s = 2\pi/L$. For this function, the integral in (34) is expressed in terms of the Bessel function $J_l(x)$:

$$f_l(K_x) = J_l(aK_x). \quad (46)$$

For large values of the amplitude one has $|f_l(K_x)|^2 \propto 1/a$ which, again, is in agreement with the estimate given before for the general case.

4 Numerical analysis of the spectral-angular density

For the numerical analysis of the radiation intensity we will study the relatively simple case when the vectors \mathbf{v} , \mathbf{e}_x and \mathbf{e}_z lie in the same plane and will consider the radiation propagating

in that plane (the vector \mathbf{k} is in the plane formed by \mathbf{v} and \mathbf{e}_x , corresponding to $\phi = 0$ and $\phi = \pi$). The geometry of the problem is depicted in figure 2. In this special case $W_\omega^\perp = 0$ and

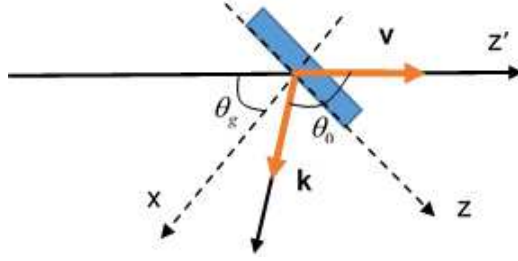


Figure 2: The geometry of the problem.

the radiation is linearly polarized: $W_\omega = W_\omega^\parallel$. The corresponding expression is given by (41) with $\phi_v = 0$ and the expression for U is simplified to

$$U = \frac{1}{\cos^2 \theta_v} \left[\frac{v g_l}{\omega} - \beta_0 \sin \theta + \left(1 - \frac{\omega_l}{\omega}\right) \sin \theta_v \right]^2 + \left(1 - \frac{\omega_l}{\omega}\right)^2 (1 - \beta_0^2). \quad (47)$$

Note that one has $\theta_v = \pi - \theta_g$, where θ_g is the charge incidence angle with respect to the normal to the boundary (x -axis). In addition, we have $\theta = \pi - \theta_g - \theta_0$, $\phi = 0$ for $\theta_0 < \pi - \theta_g$, and $\theta = \theta_0 + \theta_g - \pi$, $\phi = \pi$ for $\theta_0 > \pi - \theta_g$. In the special case under consideration, the condition (27) for the appearance of possible peaks is written as

$$\beta_0 \sin(\theta_g + \theta_0) - \sin \theta_g = l \beta_0 \frac{\lambda}{L} \left(1 - \frac{v_s}{v} \sin \theta_g\right) + \mathcal{O}(1/\gamma_0^2). \quad (48)$$

By taking into account that $v g_l / \omega = l \beta_0 \lambda / L$, we see that under this condition the expression in the square brackets of (47) is of the order $1/\gamma_0^2$ and, hence, at the peaks we have $U \sim 1/\gamma_0^2$. For a static profile one has $v_s = 0$ and (48) reduces to the condition obtained in [19] for the resonant diffraction radiation from a particle moving close to tilted grating. For $\theta_g = \pi/2$ and $v_s = 0$ one gets the standard condition for the peaks of the Smith-Purcell radiation. From (48) it follows that, for a fixed value of the incidence angle θ_g , the number of possible values of l for which the peaks appear increases with increasing L/λ . Hence, instead of a single peak in the backward transition radiation on a flat interface (in the direction of specular reflection), in the case of periodic interface one has a set of peaks. The number and the locations of the peaks depend on the incidence angle of the charge and on the periodicity properties of the interface. In the limit when the particle trajectory is parallel to the interface without crossing we get the resonance peaks of the Smith-Purcell radiation.

In figures below we plot the ratio W_ω/w_0 , with $w_0 = \alpha \hbar (\Delta \varepsilon / \varepsilon_0)^2 / \sqrt{\varepsilon_0}$ and $\alpha = q^2 / (\hbar c)$, as a function of the projection angle θ between the x -axis and the wave vector of the radiation: $k_x = k \cos \theta$, $k_z = k \sin \theta$. For the radiation propagating in the medium with permittivity ε_0 one has $-\pi/2 < \theta < \pi/2$. Recall that the validity of the approximation we used is constrained by the conditions (30). We can express these conditions in terms of the angles θ and θ_g by taking into account that $\theta_v = \pi - \theta_g$ and $\cos \theta_0 = -\cos(\theta + \theta_g)$. In particular, the approximation fails for the values of $|\theta|$ close to $\pi/2$. Note that, for a static interface, the ratio W_ω/w_0 depends on the velocity of the charge, v , and on the permittivity ε_0 through the parameter β_0 . In this case the condition for the angular locations of the peaks, for a given value of λ/L , is obtained from (48) and, up to the terms of the order $1/\gamma_0^2$, is written in the form

$$\sin \theta \approx \sin(\theta_g) / \beta_0 + l \lambda / L. \quad (49)$$

In figure 3, for the value $\beta_0 \approx 0.998694$, we have plotted the quantity W_ω/w_0 as a function of the angle θ for different values of the ratio λ/L (numbers near the curves). For $\varepsilon_0 = 1$ this value of β_0 corresponds to the electron energy $E_e = 10$ MeV. Figure 3a corresponds to the profile function (43) with $b = L/2$ and Fig. 3b corresponds to the function (45) with $\omega_s = 0$. The dashed curves correspond to the radiation on a flat boundary ($a = 0$). For the incidence angle with respect to the normal and for the ratio a/L we have taken $\theta_g = \pi/4$ and $a/L = 0.5$. It can be checked that the angular locations of the peaks for the graphs presented in figure 3 are well described by the formula (49). For example, in the case of the radiation on the triangular grating at the wavelength corresponding to $\lambda/L = 0.5$ the angular density of the radiation intensity is maximum around the angle $\theta \approx -0.91$ which is obtained from (49) for the order of diffraction $l = -3$. For the radiation with $\lambda/L = 0.5$ the maximum is around $\theta \approx -0.3$ and corresponds to the order of diffraction $l = -1$. Note that for the latter case there are no peaks for $l \neq -1$.

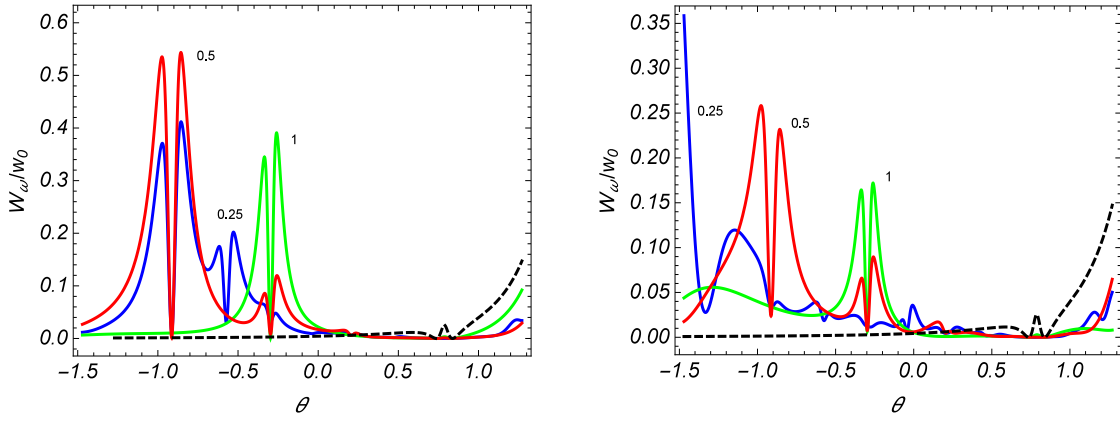


Figure 3: The spectral-angular density of the radiated energy, as a function of the radiation angle, for $\beta_0 \approx 0.998694$ (the electron energy 10 MeV in the case $\varepsilon_0 = 1$) and for separate values of the ratio λ/L (numbers near the curves). Figure 3a corresponds to the profile function (43) with $b = L/2$ and Fig. 3b corresponds to the function (45) with $\omega_s = 0$. The dashed curves correspond to the radiation on a flat boundary. The graphs are plotted for $\theta_g = \pi/4$ and $a/L = 0.5$.

Figure 4 presents the same graphs as in figure 3 for $\beta_0 \approx 0.999948$. In the case $\varepsilon_0 = 1$ the latter corresponds to the electron energy $E_e = 50$ MeV. As is seen, in accordance with the analytic estimate given above, with the increase of the energy the heights of the peaks increase by the factor γ_0^2 , whereas the widths decrease by the factor γ_0 . For $\gamma_0^2 \gg 1$, the angles around which the peaks are located are not sensitive to the value of β_0 and they are approximately the same as those for 3.

Figure 5 displays the dependence of the spectral-angular density of the radiated energy on the ratio λ/L for the function (43) with $b = L/2$ (full curves) and for the function (45) with $\omega_s = 0$ (dashed curves). The graphs in Fig. 5a and 5b are plotted for the radiation angles $\theta = 0$ and $\theta = -5\pi/12$, respectively. For both cases $\beta_0 \approx 0.998694$ (the electron energy $E_e = 10$ MeV in the case $\varepsilon_0 = 1$), $\theta_g = \pi/4$ and $a/L = 0.5$. Again, we can see that the values of the radiation wavelengths around of which the peaks are located are well described by the formula (49). In particular, for the peak with the maximal value of the wavelength one has $\lambda \approx L|\sin \theta - \sin(\theta_g)/\beta_0|$.

The same graphs, as in the right panel of figure 5, are plotted in Fig. 6 for the values $a/L = 1$ (Fig. 6a) and $a/L = 2$ (Fig. 6b). As is seen from the figures, the difference of the wavelengths for

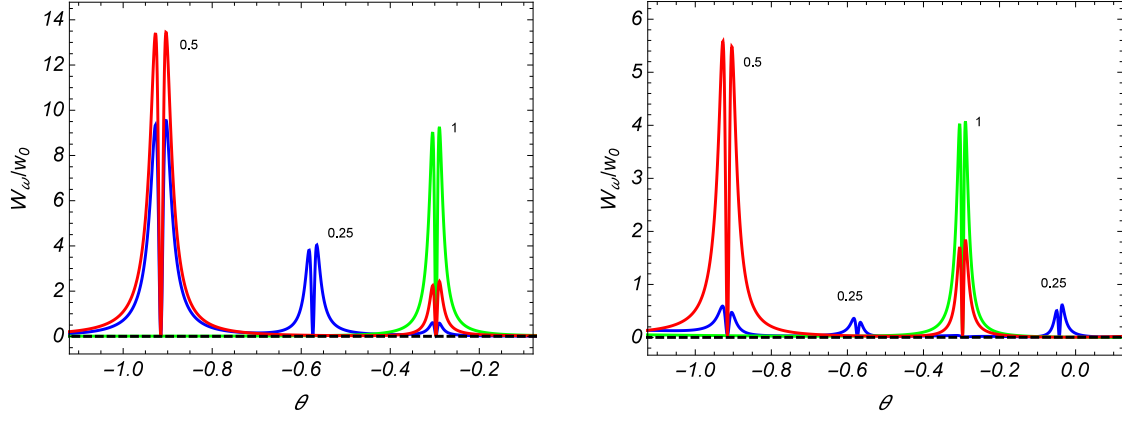


Figure 4: The same as in figure 3 for $\beta_0 \approx 0.999948$ (the electron energy 50 MeV in the case $\varepsilon_0 = 1$). The numbers near the curves correspond to the values of λ/L .

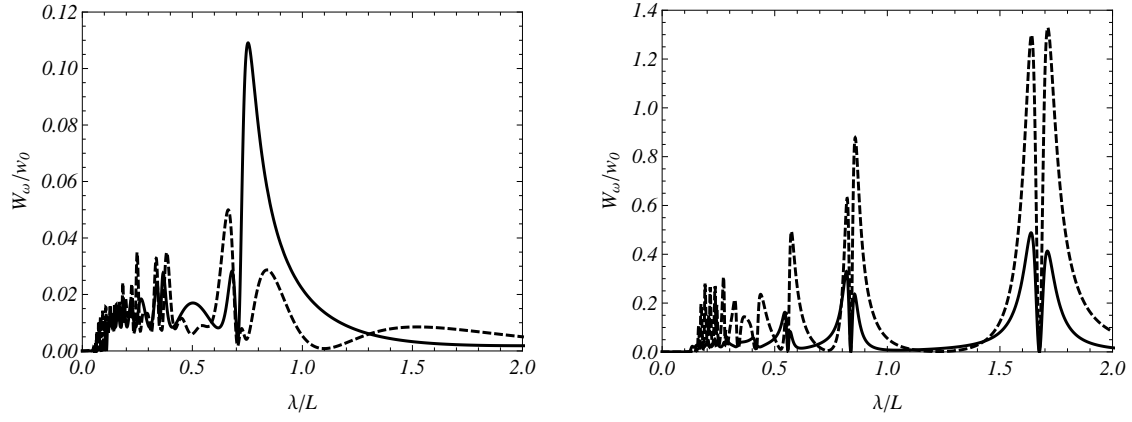


Figure 5: The dependence of the spectral-angular density of the radiated energy on the ratio λ/L for the radiation angles $\theta = 0$ (Fig. 5a) and $\theta = -5\pi/12$ (Fig. 5b). The graphs are plotted for the function (43) with $b = L/2$ (full curves) and for the function (45) with $\omega_s = 0$ (dashed curves). The values of the other parameters are the same as in figure 3.

the neighboring peaks decreases with decreasing wavelength. This is in agreement of the general estimate (49) for the spectral-angular locations of the peaks. The right peaks correspond to first order of diffraction $l = -1$.

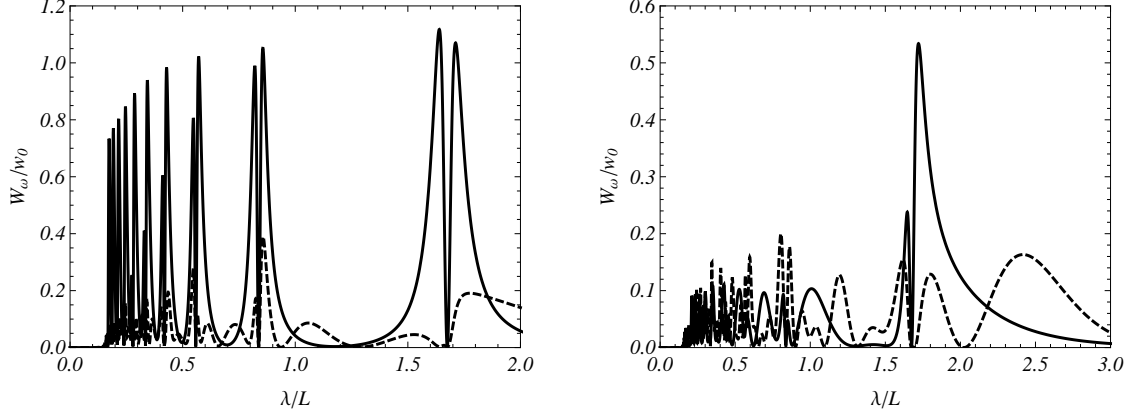


Figure 6: The same as in Fig. 5b for $a/L = 1$ (Fig. 6a) and $a/L = 2$ (Fig. 6b).

The radiation intensity at the peaks is mainly determined by the factors $|f_l(\omega K/v)|^2$ and U^{-2} in (41). As is seen from (34), the function $f_l(K_x)$ depends on the amplitude a of the function $x_0(z)$ in the form of the dimensionless combination aK_x . Hence, the dependence on the amplitude enters in the expression for the radiation intensity through the function $h_l(a\omega K/v) = |f_l(\omega K/v)|^2$. By taking into account the expression (39), for the special case under consideration corresponding to $\phi_v = 0$, the argument of the function $h_l(u)$ in the expression for the radiation intensity is presented as

$$aK \frac{\omega}{v} = -\frac{2\pi a}{L \cos \theta_g} \left\{ \frac{L}{\lambda} [1/\beta_0 + \cos(\theta + \theta_g)] + l \sin \theta_g \right\}. \quad (50)$$

For the profiles we have discussed in numerical examples, the expressions for the function $h_l(u)$ directly follow from (44) and (46). In figure 7, the functions $h_l(u)$ are plotted for the profiles (43) with $b = L/2$ (full curve) and (45) (dashed curve) in the case $l = -1$. The graphs for higher orders of diffraction have a similar structure. The values for $|u|$, at which the function $h_l(u)$ takes its first maximum (with respect to $u = 0$), increases with increasing $|l|$, whereas the value of the function at the maximum decreases. Let $u = u_l$ is the maximum point of the function $h_l(u)$ for a given l . Now, from the analysis given above, it follows that the maximal radiation intensity at the peaks, determined by the condition (48), is obtained for the values of the amplitude given by $a = vu_l/(\omega K)$. An explicit expression in terms of the angles θ and θ_g is obtained by taking into account (50). Note that, at the peaks, we can exclude the ratio λ/L from the corresponding expression by using the relation (48). In the case of the profile function (45), u_l coincides with the first zero of the function $J'_l(u)$. In particular, for $l = -1$ one has $u_l \approx 1.84$. With this value of u_l and for $\theta_g = \pi/4$, $\theta = -5\pi/12$, $\beta_0 \approx 0.998694$, the maximum radiation at the peaks is obtained for $a \approx 0.5$. This case corresponds to the dashed curve in Fig. 5b. For the triangular profile with $b = L/2$, in the case of diffraction order $l = -1$ one has $u_l \approx 4.3$ and for the same values of the parameters θ_g , θ , β_0 , the maximum radiation at the corresponding peak is realized for $a \approx 1.2$. The corresponding graph for the spectral density is similar to the full curve in Fig. 6a.

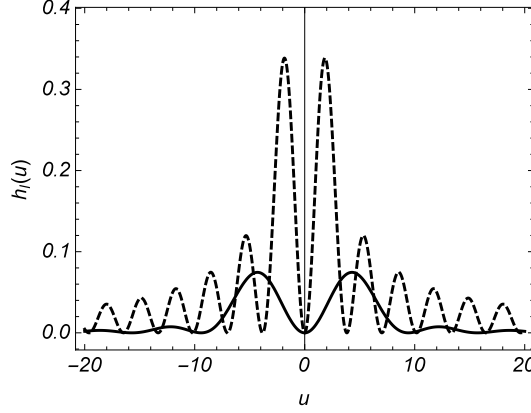


Figure 7: The function $h_l(u)$ for $l = -1$ in the expression for the spectral-angular density of the radiated energy in the cases of the triangular (with $b = L/2$, full curve) and sinusoidal (dashed curve) profiles.

5 Conclusion

We have considered transition radiation of a charged particle on an interface of two dielectric media having an arbitrary non-stationary profile. The exact solution of this problem is complicated and we have employed an approximate scheme which assumes that the dielectric permittivities of the media are close. With this assumption, the spectral-angular densities of the radiated energy on separate polarizations are given by Eq. (21) and the total radiated energy is determined by Eq. (22). The dependence on the geometry of the separating boundary enters in these expressions through the functions $f_{mnl}(K_x)$ which are the coefficients of the Fourier expansion of the function $e^{iK_x x_0(y,z,t)}$. For high-energy particles strong peaks may appear in the spectral-angular density of the radiated energy. The locations of the peaks are determined by the condition (27). This condition is completely determined by the periodicity properties of the interface and does not depend on the specific form of the profile function.

The general expressions for the radiated energy are simplified in a special case of the profile function given by (32). In this case the triple summation is reduced to the single one and the corresponding formulas are obtained by the replacements (35). A physical realization of this sort of profile function could be a surface wave excited on the boundary between two media. In terms of the spherical angular coordinates for the vectors \mathbf{k} and \mathbf{v} , the expressions for the radiated energy are presented in the form (38) and (41). As examples, in the numerical evaluation we have considered two special cases of the profile function $x_0(u)$: triangular grating with the parameters displayed in figure 1 and sinusoidal profile. Keeping in mind applications for beam diagnostics, in the numerical evaluation we have investigated the backward radiation for these two examples. Instead of a single peak in the backward transition radiation on a flat interface, for periodic interface one has a set of peaks. The number and the locations of the peaks depend on the incidence angle of the charge and on the period of the interface. The heights of the peaks in the spectral-angular distribution increase with increasing energy of the radiating particle as γ_0^2 , whereas the widths decrease as $1/\gamma_0$. The results above show that the periodic structure on the interface may serve as an additional tool for the control of spectral-angular distribution of the backward transition radiation. The corresponding features may be useful in beam and surface diagnostics.

References

- [1] M. L. Ter-Mikaelian, *High Energy Electromagnetic Processes in Condensed Media* (Wiley Interscience, New York, 1972); G. M. Gharibian and S. Yan, *Rentgenovskoye Perekhodnoye Izlucheniye* (Izd. AN Arm. SSR, Yerevan, 1983); V. L. Ginzburg and V. N. Tsytovich, *Transition Radiation and Transition Scattering* (Adam Hilger, Bristol, 1990); P. Rullhusen, X. Artru and P. Dhez, *Novel Radiation Sources Using Relativistic Electrons* (World Scientific, Singapore, 1998); A. P. Potylitsin, *Electromagnetic Radiation of Electrons in Periodic Structures* (Springer, Berlin, 2011).
- [2] A. H. Lumpkin, R. J. Dejus, and N. S. Sereno, Phys. Rev. ST Accel. Beams **12**, (2009) 040704; L. G. Sukhikh, G. Kube, S. Bajt, W. Lauth, Yu. A. Popov, and A. P. Potylitsyn, Phys. Rev. ST Accel. Beams **17**, 112805 (2014).
- [3] P. Muggli, V. Yakimenko, M. Babzien et al., Phys. Rev. Lett. **101**, 054801 (2008).
- [4] Y.-E. Sun, P. Piot, A. Johnson et al., Phys. Rev. Lett. **105**, 234801 (2010).
- [5] H. Schlarb, Diagnostic tools for ultra-low emittance and ultra-short electron bunches. Proceedings of EPAC 2000, Vienna, p.187-191.
- [6] M. Castellano, A. Cianchi, G. Orlandi et al., Nucl. Instrum. Methods A **435**, 297 (1999).
- [7] A. Doria, G. P. Gallerano, E. Giovenale et al., Nucl. Instrum. Methods A **483**, 263 (2002).
- [8] G. Doucas, V. Blackmore, B. Ottewell et al., Phys. Rev. ST Accel. Beams **9**, 092801 (2006).
- [9] V. Blackmore, G. Doucas, C. Perry et al., Phys. Rev. ST Accel. Beams **12**, 032803 (2009).
- [10] R. A. Baghiyan, Pis'ma Zh. Tekh. Phys. **2**, 1025 (1976) [Sov. Tech. Phys. Lett. **2**, 402 (1976)]; F. R. Arutyunyan, A. Kh. Mkhitarian, R. A. Oganessian, B. O. Rostomyan, and M. G. Sarinyan, Zh. Exp. Teor. Fiz. **77**, 1788 (1979) [Sov. Phys. JETP **50**, 895 (1979)]; R. A. Baghiyan, M. L. Ter-Mikaelian, Zh. Exp. Teor. Fiz. **81**, 1249 (1981) [Sov. Phys. JETP **54**, 666 (1981)]; R. A. Baghiyan, Phys. Rev. E **69**, 026609 (2004).
- [11] Y. Takakura and O. Haeblerlé, Phys. Rev. E **61**, 4441 (2000).
- [12] P. M. van den Berg, J. Opt. Soc. Am. **63**, 1588 (1973).
- [13] R. A. Baghiyan, Phys. Rev. E **64**, 026610 (2001).
- [14] A. R. Mkrtchyan, L. Sh. Grigorian, A. A. Saharian, A. H. Mkrtchyan, and A. N. Didenko, Izvestia AN Arm. SSR. Fizika **24**, 62 (1989); A. R. Mkrtchyan, L. Sh. Grigorian, A. A. Saharian, and A. N. Didenko, Acustica **75**, 184 (1991); A. A. Saharian, A. R. Mkrtchyan, L. A. Gevorgian, L. Sh. Grigoryan, and B. V. Khachatryan, Nucl. Instrum. Methods B **173**, 211 (2001).
- [15] L. Sh. Grigorian, A. H. Mkrtchyan, and A. A. Saharian, Nucl. Instrum. Methods B **145**, 197 (1998); A. R. Mkrtchyan, V. V. Parazian, and A. A. Saharian, Mod. Phys. Lett. B **24**, 2693 (2010); A. R. Mkrtchyan, V. V. Parazian, and A. A. Saharian, Int. J. Mod. Phys. B **26**, 1250036 (2012).
- [16] V. A. Davydov, Izv. Vyssh. Uch. Zav. Radiofizika **25**, 1429 (1982) [Radiophysics and Quantum Electronics **25**, 1010 (1982)].

- [17] V. A. Davydov, Zh. Exp. Teor. Fiz. **80**, 859 (1981) [Sov. Phys. JETP **53**, 437 (1981)].
- [18] V. S. Malyshevsky and I. A. Ivanova, Sov. Tech. Phys. Lett. **41**, 107 (2015); V. S. Malyshevsky, G. V. Fomin, and I. A. Ivanova, Nucl. Instrum. Methods B **359**, 75 (2015).
- [19] A. P. Potylitsyn, P. V. Karataev, and G. A. Naumenko, Phys. Rev. E **61**, 7039 (2000).